Ultrasonics Sonochemistry 92 (2023) 106246

Contents lists available at ScienceDirect

Ultrasonics Sonochemistry

journal homepage: www.elsevier.com/locate/ultson

High energy dissipation-based process to improve the rheological properties of bentonite drilling muds by reducing the particle size

Hae Jin Jo [a,1], Sung Hyun Hong [b,1], Byung Min Lee [c], Young Ju Kim [a,*], Wook Ryol Hwang [c,*], Soo Young Kim [b,*]

[a] Korea Institute of Geoscience and Mineral Resources, 905 Yeongilman-daero, Heunghae-eup, Buk-gu Pohang-si, Gyeongsangbuk-do 37559, Republic of Korea
[b] Department of Materials Science and Engineering, Institute of Green Manufacturing Technology, Korea University, 145 Anam-ro, Seongbuk-gu, Seoul 02841, Republic of Korea
[c] School of Mechanical Engineering Gyeongsang National University Gajwa-dong 900, Jinju 52828, Republic of Korea

ARTICLE INFO

Keywords:
Ultrasonic treatment
Homogenizer process
Nano bentonite
Drilling mud
Nano fluid

ABSTRACT

Drilling mud is a multi-phase fluid that is used in the petroleum drilling process. Bentonite is the most important constituent of drilling mud; it endows the drilling mud with its rheological behaviors, such as viscosity, yield stress, and shear thinning. The process of manufacturing microscale bentonite at the nanoscale level is very promising for commercializing nano-based drilling mud. In contrast to the conventional method using the impeller, bentonite was manufactured in its nanoparticle state in the present work through ultrasonic and homogenizer processes in the solution state. In case of the ultrasonic process, the viscosity increase in the low shear rate region before and after processing of the 5 wt% bentonite-based mud and the rheological properties in the presence of polymer additive were compared. In case of the homogenizer process, the rheological properties of 3 wt% bentonite-based mud employed through the homogenizer process and 5 wt% mud prepared generally were compared. Both processes reported improvement of rheological properties, in which shear thinning behavior strongly occurred when particle size decreased through FE-SEM, TEM image analysis, and particle size analyzer. A regularized Herschel-Bulkley model suitable for rheological quantitative explanation of drilling mud including yield stress was selected. The homogenizer process has the potential to be applied in the petroleum drilling industry for large-scale production, and the mechanism was confirmed by numerical analyses. In conclusion, we presented a simple and easy-to-apply process to rapidly produce nano-based drilling mud.

1. Introduction

Drilling mud refers to a non-Newtonian fluid used in the petroleum drilling process. Other applications include transport cuttings, pressure-maintenance of bore holes, filter cake formation, and bit lubrication and cooling [1,2]. Drilling mud is divided into water-based drilling mud (WBM), oil-based drilling mud (OBM), and synthetic-based drilling mud (SBM). OBM consist of dearomatized oils, wetting agents, filtrate-reducing agents, lime, emulsifiers, clays, viscosifying agents, and brine of varying concentrations [3]. SBM systems are formulated as an emulsion in which the synthetic liquid forms the continuous phase while a brine serves as the dispersed phase. It allows more environmentally acceptable drilling than oil-based muds for use in offshore drilling [4]. OBM and SBM perform better than WBM; however, they have environmental problems to some extent and are expensive [5]. The environmental issues associated with the use of oil-based fluids have restricted or banned their use in certain locations [6]. WBM is the most widely used drilling mud because it is easy to fabricate, has relatively low maintenance costs, and can be formed to overcome most problems associated with drilling operations [7]. WBM, which are composed of bentonite, barite, and polymers [8–10], have the advantage of being eco-friendly.

Drilling mud is generally composed of a particle suspension based on bentonite particles and can be classified as a rheologically complex fluid with a microstructure. The shear thinning phenomenon occurs according to the house of the card structure in the static state of bentonite [11]. Drilling mud is characterized by a strong interdependence between thixotropy and temperature. Because it is a viscoplastic fluid containing

* Corresponding authors.
E-mail addresses: kyjp7272@kigam.re.kr (Y.J. Kim), wrhwang@gnu.ac.kr (W.R. Hwang), sooyoungkim@korea.ac.kr (S.Y. Kim).
[1] Hae Jin Jo and Sung Hyun Hong prepared equally experiment and wrote the original manuscript.

https://doi.org/10.1016/j.ultsonch.2022.106246
Received 26 August 2022; Received in revised form 17 November 2022; Accepted 25 November 2022
Available online 28 November 2022

yield stress, shear thinning is dominant, particularly at low shear, and its physical properties change when it is subjected to flow or deformation [12]. Owing to its rheological properties, it is used in various applications such as transportation, cutting of rocks, cooling, and supporting of equipment through pressure formation. Viscosity during drilling operations is an important drilling fluid property because it has a profound effect on frictional pressure loss, pump pressure, and solids sedimentation rate [13]. In its stationary state or at a low shear rate, mud must have high-viscosity characteristics and high yield stress such that crushed rock fragments are suspended in support and drilling equipment to avoid sedimentation [14]. Failure to support rock fragments and drilling rigs can cause circulation losses, high rotational torques, and excessive bit wear [15]. At a high shear rate, mud transportation through the internal circulation of a drilling rig or through its pipeline, where low viscosity is required to reduce the power requirement [16], is necessary. Owing to the role played by the drilling mud, a high viscosity is required at a low shear rate (little or no flow), and a low viscosity is required in the case of a high shear rate with a high flow rate. Therefore, drilling muds with strong shear thinning behavior can be considered optimal, and it is essential in the drilling industry to precisely control the rheological properties of drilling mud.

As oil wells on land are gradually depleted, the frequency of drilling in extreme environments is increasing, and the performance of drilling mud must be further improved [17]. Various studies have been conducted to improve the properties and performance of drilling mud, and recently, manufacturing nano-based drilling mud has been in the spotlight. Nanoparticles have special characteristics such as small size (1–100 nm), high specific surface area, and a high ability for adsorption [18]. Nano-based drilling mud has been a solution to overcome the limitations of existing drilling mud [19]. Various studies have been conducted to investigate increasing the specific volume of particles to have a higher viscosity for the same mass [20,21], reducing the fluid loss through easier filter cake formation [22], the endurance to extreme environments such as high temperature and high pressure [23], and increasing the thermal conductivity [24]. However, because nanoparticles still have problems in their commercialization owing to associated costs, research on the mass production of nanoparticles is necessary.

Bentonite is the most important material in drilling mud; it endows drilling mud its viscosity, yield stress, shear thinning properties [11]. Because it is advantageous in terms of price compared to other nano particles, studies have reported that bentonite can be made at a nano scale to improve its performance as a drilling mud [25]. The ball milling process is the most common process for manufacturing nano bentonite, but it takes a long time and has the disadvantage of separating samples after the dispersion process [26]. The ultrasonic manufacturing method is a process in which nanoparticles can be produced by applying a temperature of 5000 °C and pressure of 500 bar to a local portion of the solution [27]. Darvishi et al. manufactured bentonite in the form of nanorods using an ultrasonic process [28]. However, because the study was not applied to drilling mud, we designed similar conditions and conducted an experiment to address issue. As a result, we succeeded in producing nano-bentonite in a short time. Although the ultrasonic processing time was short, there were several limitations. It was possible to efficiently manufacture nanoparticles only when ultrasonic treatment was performed 24 h after mixing bentonite, and the concentration of bentonite was limited, which is disadvantageous for the mass production of nano bentonite. (Fig. 1a). To improve this process, we introduced a homogenizer. When a homogenizer is used, 24 h waiting period is not required after mixing bentonite (Fig. 1b). Furthermore, it can also be applied to high-concentration bentonite solutions, which is advantageous for the mass production of nano-bentonite in a short period of time. In this paper, we present a process for producing nano bentonite through both ultrasonic and homogenizer processes, as well as an analysis of the physical properties of drilling mud.

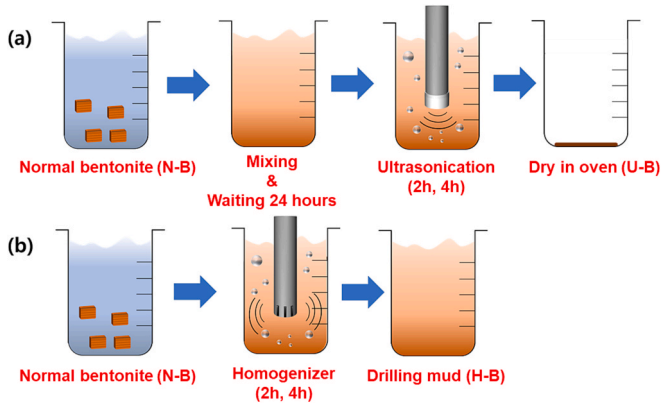

Fig. 1. Schematics of manufacturing bentonite-based mud through the experiments (a) the ultrasound process, (b) the homogenizer process.

2. Experimental details

2.1. Chemical materials

Xanthan gum (Sigma Aldrich) was purchased and used as received, that is, without further purification. The bentonite acquisition was supported by Clariant Korea.

2.2. Normal bentonite based drilling mud

The manufacture of drilling mud generally follows the American Petroleum Institute Specification 13A (API). According to the API specifications, the process is as follows. (1) The material is prepared and (2) mixed, (3) lumps are scraped from the wall of the container and mixed until they dissolve, (4) and then the contents are sealed and stored. After storage, the mud is mixed for a few minutes to stabilize it, and the rheological properties are measured. Deionized water (DI water) and bentonite were mixed with drilling mud to minimize the influence of other factors. Drilling mud composed of only normal bentonite was mixed with DI water at a concentration of 5 wt%, and the drilling mud in which xanthan gum was added was mixed with 5 wt% bentonite and 0.4 wt% xanthan gum.

2.3. Synthesis of nano bentonite by ultrasonication

Normal bentonite was mixed in DI water at a concentration of 1.25 wt%, sealed for 24 h, and then stabilized. A pulse of ultrasonic waves was applied at an intensity of 60 W for 3 s, followed by rest for 2 s, and each sample was treated for 2 h and 4 h. In the actual experiment, the energy rate was calculated to be 250 kJ in 400 mL solution per hour. During ultrasonic treatment, the bentonite solution was maintained at 4 °C by using chiller. After the treatment, the bentonite in the DI water was dried and powdered.

2.4. Synthesis of nano bentonite by homogenizer

A rotor–stator was used for the rotating part of the homogenizer to mix the drilling mud based on bentonite, and the process was performed at the high rotational speed of 6000 rpm. The top view and dimensions of the rotor–stator used are shown in Fig. 2(a); the stator diameter (D_1) was 40.6 [mm], rotor diameter (D_2) was 33 [mm], stator gap (C_1) was 1.3 [mm], rotor gap (C_2) was 1.4 [mm], and gap between the rotor and stator C_3 was 0.8 [mm]. The three-dimensional structure of the rotor–stator type homogenizer is shown in Fig. 2(b). As shown in Fig. 2(b), multiple shear gaps are formed by the stator and rotor, which causes strong turbulent shear stress, and turbulent jets are formed along the stator gap to disperse the particles. We selected the vessel diameter (T)

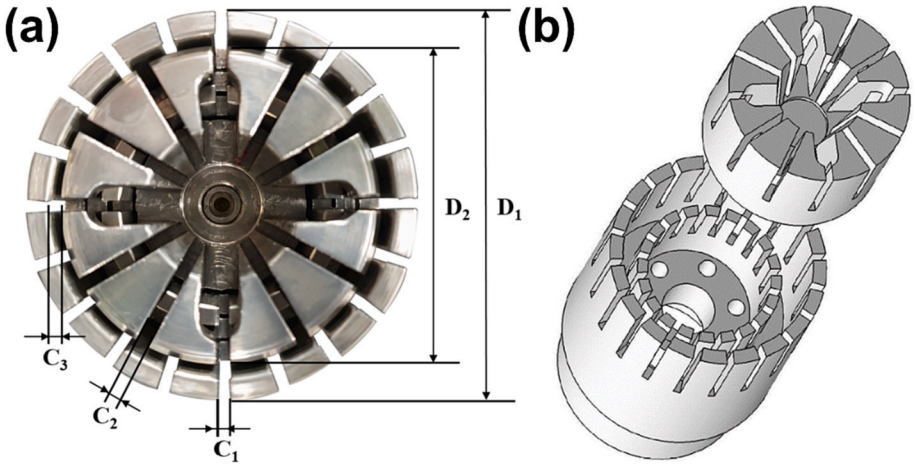

Fig. 2. Schematic images of the configuration of homogenizer (a) images of a rotor–stator type homogenizer and its (b) inner structure.

75.8[mm], and the gap between the vessel wall and the stator is not large and a half of the rotor diameter. The mixing effect using a homogenizer with a small gap between the wall of the vessel is increased compared to the case of a wide gap between the wall of the vessel and the stator, since flow strength or the mean energy dissipation rate increase with reduction of the vessel size. However, too small vessel yields significant local viscous heating with drilling muds. A stainless-steel vessel was selected because if a strong shearing force is generated at a high rotational speed, scratches or other forms of damage may occur on the vessel. In the manufacturing process, the amount of bentonite (Clariant Korea, Seoul, Korea) and distilled water at the desired weight percent were measured, placed in a container, and the rotation speed was set to 6,000 rpm, followed by mixing by rotating the homogenizer. To compare the mud with improved rheological properties using a homogenizer, the drilling mud was manufactured according to API specifications using the 4-blade PBT45 (pitched bladed turbine, 45°) impeller, which is the most commonly used impeller. The dimensions of the used PBT45 were as follows: the ratio of the impeller diameter to the vessel diameter (D/T) was 0.76, ratio of the impeller height to the vessel diameter (H/T) was 0.17, ratio of the clearance between the impeller and vessel diameters to the vessel diameter (C/T) was 0.12, and ratio of the width to the diameter of the impeller (W/D) was 0.30. When the mixing was completed, the drilling mud was sealed and aged at room temperature for more than 48 h and then mixed using PBT45 for approximately 5 min to stabilize it; precipitation occurred evenly (Fig. 1b).

2.5. Characterization

FE-SEM images were obtained using a field-emission scanning electron microscope (Zeiss 300VP) at an acceleration voltage of 5 kV. TEM images were obtained using a JEOL transmission electron microscope. The surface charge of the bentonite particles was measured using zeta potential (Otsuka ELSZ-1000). The thermal conductivity (KD2 pro) of the drilling mud was measured using the transition hot wire method [29]. Ultrasonicator (SONICS VCS0750, 20 kHz, compressive wave, Sonics & Materials) was used to fabricate nano bentonite in solution process. A rheometer was used to measure the viscosity and shear stress according to the shear rate of drilling mud (MCR301, Anton Paar). A particle analyzer was used to measure the particle size and distribution of the drilling mud through laser diffraction technology (Mastersizer 3000, Malvern Panalytical).

3. Results and discussion

3.1. Synthesis of nano scale bentonite using an ultrasonic process

In this study, a total of seven different drilling muds were prepared:3 and 5 wt% bentonite based muds (*N*-B 3 wt%, N-B 5 wt%), mud composed of 5 wt% bentonite and 0.4 wt% xanthan gum (*N*-B 5 wt% +X. G. 0.4 wt%), 5 wt% bentonite based muds with 2 and 4 h of ultrasonication {U-B (2 h) 5 wt%, U-B (4 h) 5 wt%}, and 3 wt% bentonite based muds with 2 and 4 h homogenizer process{H-B (2 h) 3 wt%, H-B (4 h) 3 wt%}. It has been reported that drilling mud exhibits non-Newtonian fluid behavior and yield stress when the concentration of bentonite exceeds 1 wt% [8], and all drilling muds used in this study showed viscoplastic behavior, including yield stress.

Field emission scanning electron microscopy (FE-SEM) measurements were conducted to confirm the size and morphology of the bentonite. It was confirmed that the particle size of N-B was several micrometers (Fig. 3a), whereas in the case of bentonite produced through ultrasonic treatment, the particle size decreased with time, and the particle shape was a general 2-d structure (Fig. 3b, c), as in previous research [30]. Transmission electron microscopy (TEM) was performed to confirm the size of the smaller bentonite particles, and by comparing the TEM images before and after ultrasonic treatment, it was confirmed that even the smallest N-B particles exceeded 1 μm (Fig. 3d), while the bentonite treated using the 4 h ultrasonic process was reduced to tens of nanometers (Fig. 3e). A particle size measuring device based on laser diffraction technology was used to confirm the overall change in the particle size through the size distribution of bentonite. Because bentonite is a swelling material [31], the particle size distribution measured in the solution was approximately 10 times larger than that of bentonite measured by FE-SEM and TEM. The particle size distribution data confirmed that the size distribution of bentonite was significantly reduced as the duration of the ultrasonic treatment increased (Fig. 3f). Detailed particle size distribution results are presented in Table S1.

3.2. Rheological properties of nano scale bentonite using the ultrasonic process

For 3 wt% and 5 wt% drilling muds, the effects of bentonite concentration on rheological properties are compared. For the case of mud with 0.4 wt% xanthan gum added to 5 wt% mud, xanthan gum, which is commonly used as a thickener, is added to analyze the effect of the polymer. The mud manufacturing process with a thickener, which is commonly used to improve viscosity, can be used as a reference for comparison with the process that uses ultrasonic waves for normal drilling mud that only has bentonite.

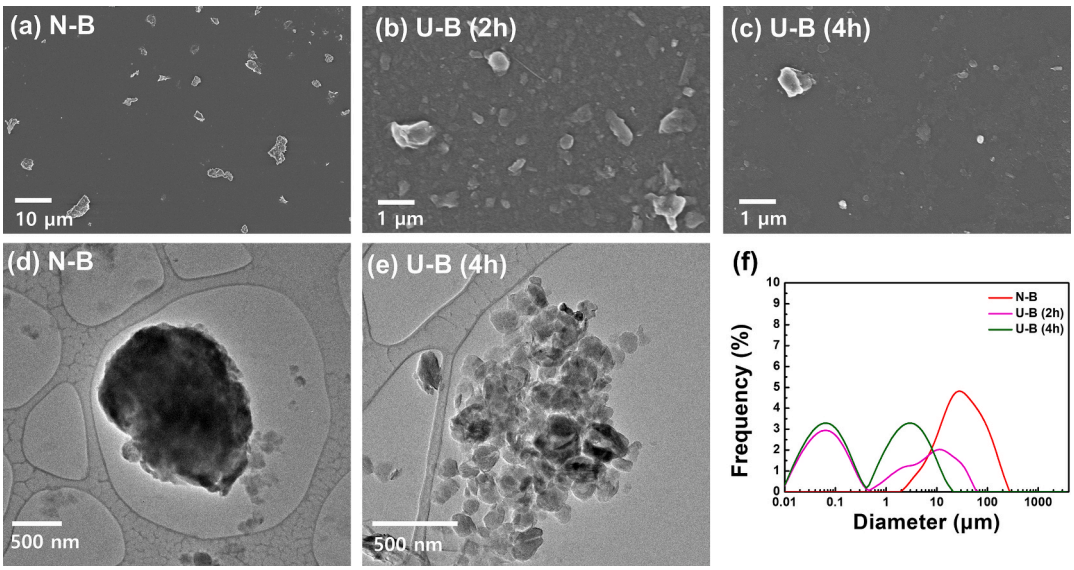

Fig. 3. Bentonite processed using ultrasonic treatment. (a) FE-SEM images of normal bentonite (*N*-B), (b) bentonite with ultrasonic treatment for 2 h (U-B 2 h), bentonite with ultrasonic treatment for 4 h (U-B 4 h), (d) TEM images of N-B, (e) U-B 4 h, (f) size distribution of N-B, U-B 2 h, and U-B 4 h.

Fig. 4 shows rheological properties of 5 wt% normal bentonite based drilling mud, mud with 0.4 wt% xanthan gum as an additive, and 5 wt% normal muds that were subjected to ultrasonic processes for 2 h and 4 h, respectively. By precisely measuring viscosity through a rheometer, the viscosity behavior according to the shear rate of drilling mud manufactured by applying various processes was obtained, as shown in Fig. 4 (a).

The rheological properties of drilling mud, which is a non-Newtonian fluid that exhibits shear thinning behavior by changing the viscosity according to the applied shear rate, were measured in the range 0.008–1000 [1/s] through the shear rate using a rheometer at 20 °C under the same conditions. The predictive nature of recently developed rheological models can be incorporated to improve rheological characterization of drilling muds with nanoparticles [32] To quantitatively compare the measurement results of the rheological properties of drilling mud, an explicit viscosity model that can be expressed as a function of shear rate was introduced, and the regularized Herschel-Bulkley model [33] in Eq. (1) was employed:

$$\mu(\dot{\gamma}) = \tau_y(1 - e^{-m\dot{\gamma}})/\dot{\gamma} + k\dot{\gamma}^{n-1} \quad (1)$$

The regularized Herschel-Bulkley model is suitable for expressing the viscosity behaviors of mud in the presence of yield stress, τ_y, and facilitates straightforward numerical simulations of yield stress fluids [34]. In Eq. (1), k is the consistency index, n is the power-law index, and m is a stiffness parameter. The curve-fitted rheological properties of all drilling muds used in this study are presented in Table 1.

Fig. 4(b) shows the measured mud viscosity behavior obtained by curve fitting using the regularized Herschel-Bulkley model. From the measurement results of the rheological properties shown in Fig. 4(a) and (b), it can be observed that the viscosities of the mud with a thickener (xanthan gum) and mud subjected to an ultrasonic process are both higher than that of the 5 wt% normal mud with the same concentration over the entire shear rate range. When xanthan gum was added to the 5

Table 1
Curve-fitted rheological properties of all drilling muds.

	τ_y[Pa]	m [s]	k [Pa • s^n]	n[−]
N-B 3 wt%	0.747	100	0.0632	0.699
N-B 5 wt%	4.524	1000	3.142	0.278
N-B 5 wt% + X.G. 0.4 wt%	17.398	1000	4.290	0.282
U-B (2 h) 5 wt%	14.346	1000	2.815	0.265
U-B (2 h) 5 wt%	22.870	1000	3.854	0.225
H-B (2 h) 3 wt%	2.252	1000	0.275	0.390
H-B (4 h) 3 wt%	4.936	1000	0.350	0.312

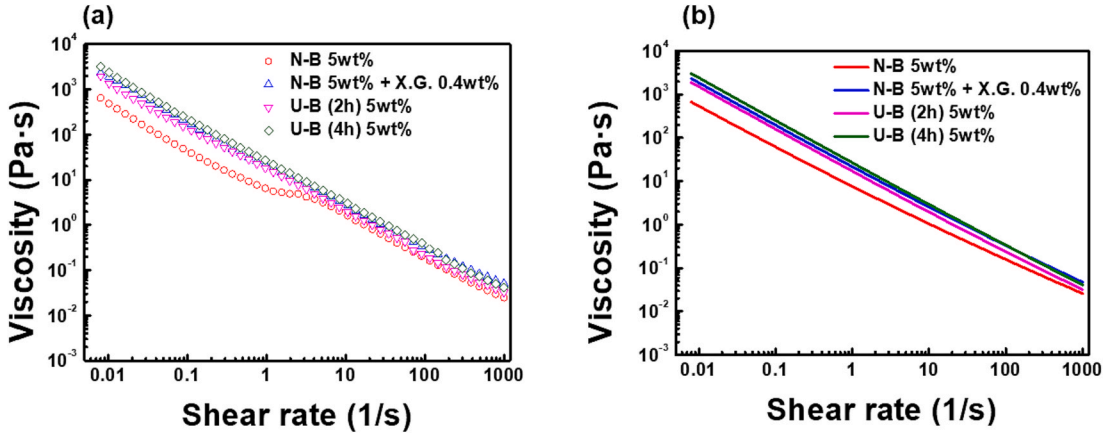

Fig. 4. Viscosity as a function of the shear rate for the four different drilling muds manufactured by ultrasonic treatment. (a) Rheological properties measured by rheometer. (b) Fitted rheological properties by regularized Herschel-Bulkley model.

wt% mud, the viscosity and yield stress were higher than those of the mud treated for 2 h at low shear. However, comparing the *n* value, which indicates the slope of the shear rate-viscosity behavior, shows that the mud produced by the 2 h sonication process is lower; therefore, its shear thinning behavior is stronger than that of the mud containing xanthan gum. This can be considered a weakness because when a thickener is used, the overall viscosity increases and the *n* value increases; therefore, the shear thinning tendency is relatively weak, and the viscosity does not decrease significantly at high shear in the process of fluid transportation. However, for the mud prepared by performing an ultrasonic process on 5 wt% normal mud for 4 h, the yield stress was higher, and the *n* value was lower than those of 5 wt% normal mud and 5 wt% mud containing xanthan gum. This mud can be considered ideal owing to its high viscosity at low shear and low viscosity at high shear.

3.3. Synthesis of nano scale bentonite using homogenizer process

Fig. 5 shows the particle size and morphology of bentonite manufactured through the homogenizer process. It was confirmed that bentonite particles manufactured by this process became smaller over time, similar to those of the ultrasonic process, and it was confirmed that the size of the particles decreased to within 1–2 μm (Fig. 5a and b). The TEM images also show that the bentonite particles shrink to hundreds of nanometers in 4 h (Fig. 5c). In the bentonite particle size distribution, the change in the particle size was significantly different, and this tendency was the same as that of the ultrasonic process (Fig. 5d). As the bentonite decreased to the nanoscale, the zeta potential was measured to confirm that there were no other changes in the particle properties. It was confirmed that the surface charge of N-B was not significantly different from those of the bentonites treated using ultrasonic and homogenizer processes, and the two processes did not change any characteristics other than the size of the bentonite particles (Table S2). In addition, as the particles decreased, the change in the thermal conductivity of the drilling mud was measured, and there was a slight increase in the thermal conductivity due to the increased specific volume of the bentonite, but the increase was not significantly different from 10 % (Table S3).

3.4. Rheological properties of nano scale bentonite using the homogenizer process

Fig. 6 shows the rheological properties of mud treated with 5 wt% and 3 wt% normal muds, as well as those of mud treated with 3 wt% normal mud using homogenizer processes for 2 h and 4 h. Fig. 6(a) shows the viscosity behavior according to the shear rate of the drilling mud manufactured by applying the homogenizer process, which was precisely measured using a rheometer. Fig. 6(b) shows the results of fitting the viscosity behavior according to the shear rate measured from the mud. Based on the rheological properties shown in Fig. 6(a) and (b), the viscosity of the mud subjected to the homogenizer process for 2 h and 4 h is higher than that of the 3 wt% normal mud with a similar concentration over the entire shear rate range. In the high-shear range, the viscosity gradually converged to the result of 3 the wt% normal mud. In particular, for the 3 wt% mud subjected to the homogenizer process for 4 h, the behavior is similar to that of the 5 wt% normal mud at low shear and shows strong shear thinning, as it converges to the viscosity of the 3 wt% normal mud at high shear. For the yield stress, compared to those of the 3 wt% normal mud, the rates of increase were approximately 3 and 6.6 times higher when the homogenizer process was applied for 2 h and 4 h, respectively. Compared to that of the 5 wt% normal mud, the yield stress was higher when the homogenizer process was applied for 4 h.

The ultrasonic process was performed on a relatively small lab-scale. However, In the homogenizer process, it can be considered as an ideal process for controlling the rheological properties of mud because it is applied at an industrial scale for pilot and mass production processes, and the corresponding installation and process are simple.

3.5. Hydrodynamic mechanism of a homogenizer

Homogenizers are widely used to produce emulsions and particle dispersions in industrial processes, such as chemicals, foods, and cosmetics, owing to their scalability [35]. Homogenizers such as rotor stators are characterized by a high-speed rotor in close proximity to a stator and are called high-shear mixing devices owing to their very high shear rate, which is in the order of $10^4 \sim 10^5$/s. It has been reported that the high energy dissipation rate in the narrow gap between the stator

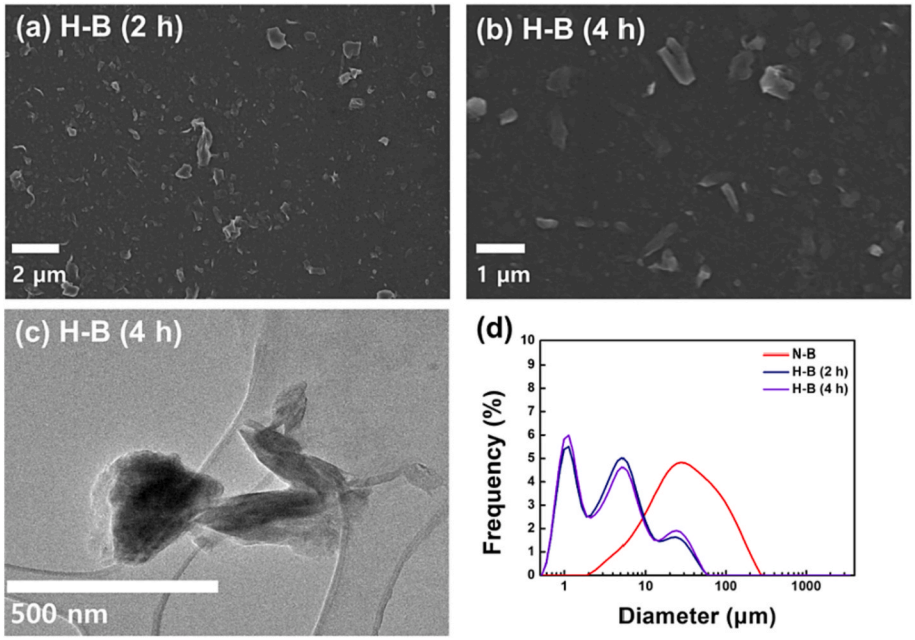

Fig. 5. Bentonite processed using a homogenizer. (a) FE-SEM images of bentonite processed using a homogenizer for 2 h (H-B 2 h), (b) bentonite processed using a homogenizer for 4 h (H-B 4 h), and (c) TEM images of bentonite processed using a homogenizer for 4 h. (d) Size distributions of N-B, H-B 2 h, and H-B 4 h.

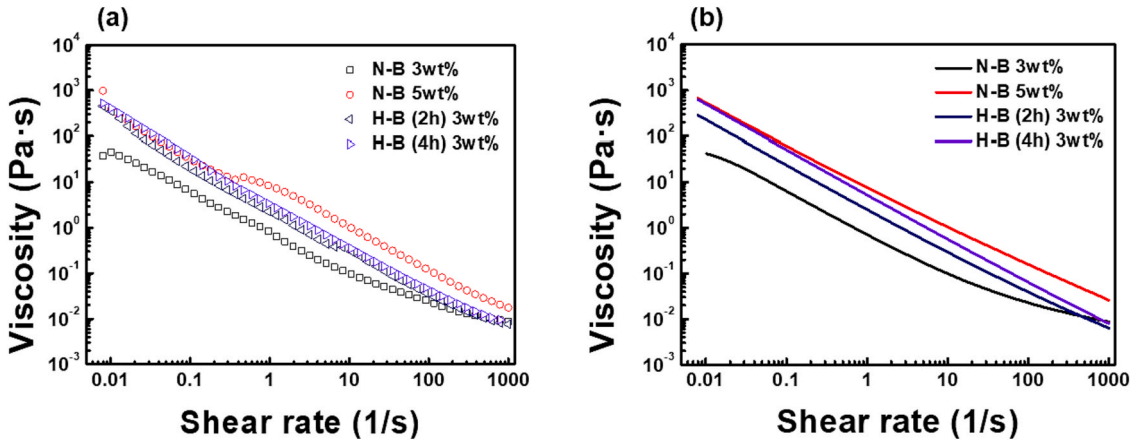

Fig. 6. Viscosity as a function of the shear rate for the four different drilling muds manufactured by homogenizer. (a) Rheological properties measured by rheometer. (b) Fitted rheological properties by regularized Herschel-Bulkley model.

and rotor contributes to the high level of turbulent kinetic energy and that the a shear gap is important for efficient dispersion [36,37].

In this study, a rotor–stator-type agitator was used, and as shown in Fig. 7(a), a strong turbulent jet formed from the narrow flow path between the rotor and stator. Owing to the decreased particle size of drilling mud in a strong turbulent jet, drilling mud with improved rheological properties can be mass-produced from nanoparticles using a homogenizer. The high-shear homogenizer process is suitable from two viewpoints compared to the process that uses an impeller. First, in the process that uses an impeller, laminar flow agitation predominantly occurs because of the high viscosity of drilling mud at low shear. On the other hand, in the case of a homogenizer, a high-shear process is

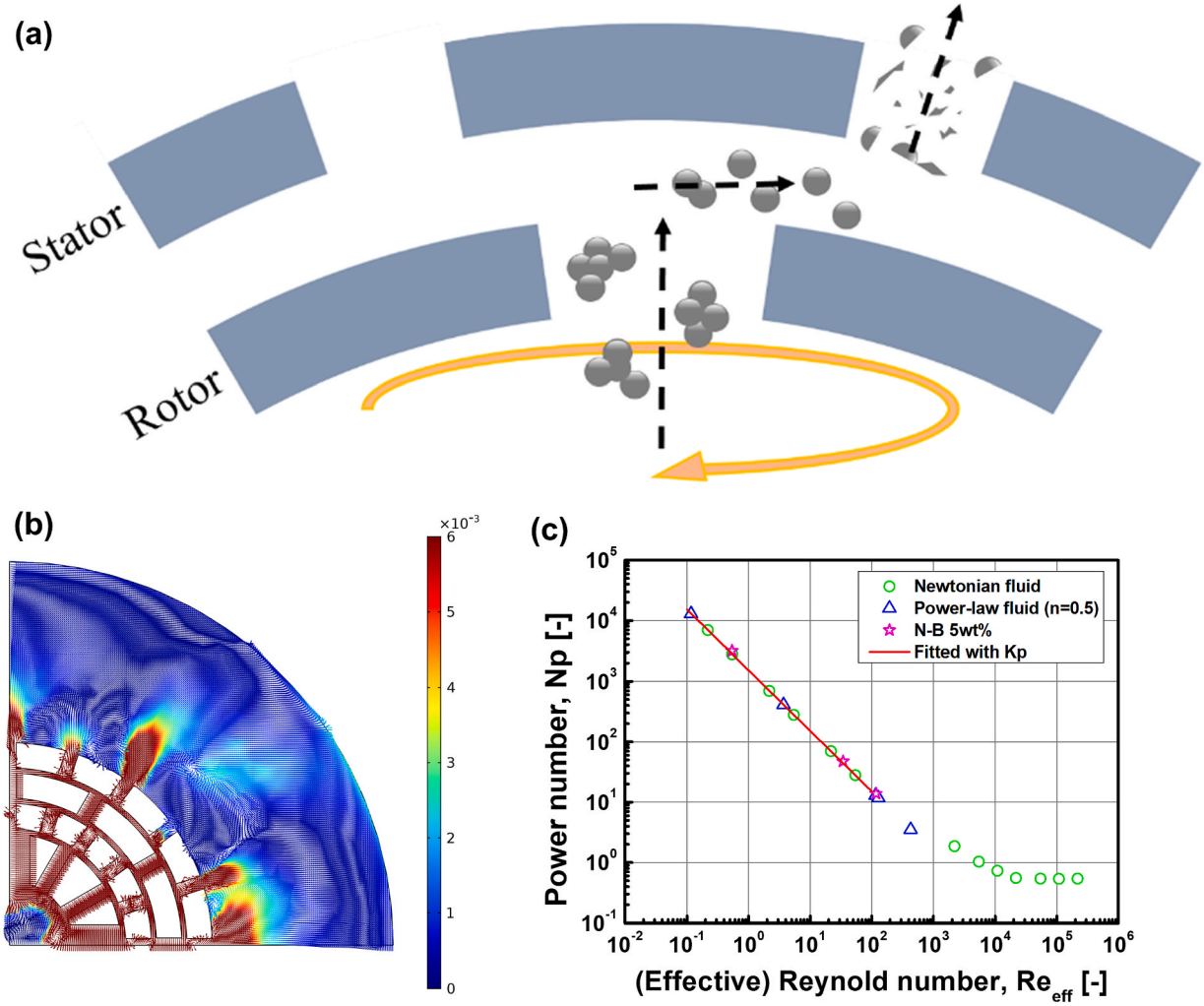

Fig. 7. Theory and analysis of homogenizer (a) schematic of the hydrodynamic mechanism of homogenizers, (b) the velocity field of the homogenizer calculated from numerical analysis, and (c) the relationship between the power number and the effective Reynolds number ($N_P - Re_{eff}$) of the rotor–stator type homogenizer.

dominant, and strong inner turbulent mixing occurs. Hence, it is possible to efficiently disperse bentonite by improving the dispersibility of bentonite agglomerates and particles through additional turbulent stress. Second, because strong turbulent eddies are generated at the microscopic scale, the liquid medium can efficiently penetrate the bentonite agglomerates and particles, yielding improved wetting of the bentonite agglomerates. As a result, the rheological properties are improved by decreasing the particle size of the bentonite constituent of the drilling mud from the turbulent jet generated by the shear gap of the homogenizer.

3.5.1. Numerical analysis result of the homogenizer

To verify the experimental results, including the turbulent jet and turbulent stress generated by the homogenizer, turbulent flow simulations were performed using COMSOL Multiphysics 5.5. The standard $k-\varepsilon$ model was used for the numerical analysis of the turbulent flow, and because the homogenizer has a periodic geometry, we analyzed only a quarter of the domain. For the boundary conditions, the rotational speed was assigned at the rotor boundaries, and rotational periodic boundary conditions were set on the sidewalls. As the rotor rotates at a high speed, the fluid inside is pushed out, and bentonite suspensions at the bottom of the homogenizer enter the homogenizer and are discharged to the outside, forming a strong turbulent jet. Therefore, we employed free-stress conditions at the upper and lower surfaces to allow the fluid to enter and leave the homogenizer. To verify the accuracy of the simulation, we performed a mesh refinement test using four different meshes. Although not presented in this paper, the relative error of the total power draw showed a uniform convergence as the number of unknowns increased. The accuracy of the flow simulation results was guaranteed for up to three significant digits.

Fig. 7(b) shows the velocity field of a 5 wt% normal drilling mud at 6000 rpm under the same conditions as those in the experiment. The velocity field shown in Fig. 7(b) is on the horizontal cross section at 2/3 of the height from the bottom. The first and third rows of teeth from the center are the rotors, and the second and fourth rows of teeth are the stators. When the first row of teeth (rotor) rotates, the flow enters narrow gaps in the second row of teeth (stator). As the flow enters and contacts the third row of teeth (rotor), a circulating flow occurs at the second row of teeth (stator). As the third row of teeth (rotor) rotates, it faces the tip of the stator farthest from the center, and a turbulent jet is emitted. The colors in the flow pattern in Fig. 7(b) indicate the dimensionless turbulent dissipation rate (ε/N^3D^2), where ε is the turbulent dissipation rate [m^2/s^3], N is the rotational speed of the rotor [rps], and D is the outer swept diameter of the rotor [m].

3.5.2. Power characteristics of the homogenizer with drilling mud

The quantification technique for agitator flow proposed by Metzner and Otto was applied to quantitatively represent the complex non-Newtonian fluid flow occurring in the homogenizer. Metzner and Otto proposed a method to quantify the complex flow of non-Newtonian fluids defined by the energy balance, in which the power supplied from the outside is dissipated by the viscosity of the laminar flow inside the system. Furthermore, they hypothesized that the effective shear rate $\dot{\gamma}_{eff}$, is proportional to the impeller rotational speed [38].

$$\dot{\gamma}_{eff} = K_S N \tag{2}$$

The Metzner-Otto constant, K_S, is a function of the geometry of the system and is almost independent of the rheological properties of the fluid.

In a Newtonian fluid, the power required by the agitator can be defined by making it dimensionless using the power number, $N_P = P/\rho N^3 D^5$, of the agitator. N_P is proportional to the reciprocal of the Reynolds number ($Re = \rho ND^2/\mu$) in laminar flow.

$$N_P = K_P/Re \tag{3}$$

Similar to the Metzner–Otto constant, K_S, the energy dissipation rate constant, K_P, is almost independent of the rheological properties of the fluid and is determined by the geometry of the system. P is the power of the agitator, ρ is the density of the fluid, N is the rotational speed of the agitator, D is the diameter of the agitator, and μ is the fluid viscosity.

According to the flow quantification technique of Metzner and Otto, in the same agitator geometry system, the power number and effective Reynolds number relationship, $N_P - Re_{eff}$, of a non-Newtonian fluid that shows shear thinning behavior can be defined using K_P.

$$N_P = K_P/Re_{eff}, Re_{eff} = \rho ND^2/\mu_{eff}, \mu_{eff} = \mu(\dot{\gamma}_{eff}) \tag{4}$$

The effective Reynolds number, Re_{eff}, of a non-Newtonian fluid can be defined through the effective viscosity, μ_{eff}, where μ_{eff} is a function of the effective shear rate $\dot{\gamma}_{eff}$ and mimics the rheological properties of the fluid.

In this study, the power, $P = 2\pi NT$, was calculated using the torque (T) generated by the rotation of the homogenizer rotor in the numerical analysis results, and the complex homogenizer flow was quantified using the power calculated by applying the Metzner-Otto method. The energy dissipation rate constant (K_P) of the rotor–stator type homogenizer used in this study, calculated from the Newtonian fluid quantification results, is 1514.793. The Metzner-Otto constant (K_S) is determined according to the geometry of the system and is almost independent of the rheological properties of the fluid. Therefore, it was calculated through a numerical analysis of a power-law fluid with $k = 10$ and $n = 0.5$, and the Metzner-Otto constant (K_S) is 144.343. The numerical analysis results of the 5 wt % normal drilling mud in the homogenizer system were quantified using the energy dissipation rate constant (K_P) and Metzner-Otto constant (K_S). Fig. 7(c) shows the relationship between the power number and the effective Reynolds number ($N_P - Re_{eff}$) of the rotor–stator-type homogenizer used in this study. The results of all fluids converge to a single curve in a laminar flow ($N_P = 1514.793Re^{-1}$), which is consistent with the $N_P - Re$ results for Newtonian fluids.

To define turbulent flow quantification, including the turbulent dissipation rate (ε) and turbulent stress of the 5 wt% normal drilling mud used in the experiment, a numerical analysis was performed at 6,000 rpm, similar homogenizer rotor speed as that for the experiment. When the density (ρ) of the 5 wt% normal drilling mud is 1075 [kg/m^3] and the rotation speed is 6,000 rpm, the effective viscosity (μ_{eff}) according to $\dot{\gamma}_{eff}$ was defined using the Metzner-Otto constant (K_S), and a numerical analysis was performed. The power number of the homogenizer mixing the 5 wt% normal drilling mud was 0.424. The average turbulent dissipation rate (ε) around the stator, that is, the fourth row of teeth, at which the turbulent jet occurs, is 1967.8 [m^2/s^3]. The volume-averaged mean size, D[4,3], which is mainly used to monitor coarse particles, such as bentonite particles of the 5 wt% normal drilling mud, is 64.7 [μm]. Because the turbulent stress can be expressed as $\tau = \rho\varepsilon^{2/3}d^{2/3}$ for the length scale (d), the average turbulent stress applied to the particles can be estimated as 272.06 [Pa] in the jet of the homogenizer rotating at 6,000 rpm.

4. Conclusion

In summary, we presented two processes, that is, ultrasonic and homogenizer processes, which are effective in replacing the conventional ball milling process for manufacturing bentonite at the nanoscale. Microscale bentonite was dispersed into nanoscale bentonites within only a few hours of processing, and in particular, the homogenizer process had the advantage of scalability, which allows a sufficient concentration to be manufactured directly as drilling mud at a large scale. In the case of U-B 5 wt% 4 h, the low shear viscosity increased before and after ultrasonication processing of the N-B 5 wt% and the rheological properties in the presence of polymer additive were quantitatively compared. In the case of drilling mud manufactured through

the ultrasonic process, unlike the case of adding polymer, it was shown that the viscosity increased at low shear and converges to the viscosity of the mud having the same weight percent at high shear. H-B 3 wt% showed a strong shear thinning behavior because it had a viscosity value similar to that of N-B 5 wt% at low shear and converged to the viscosity of N-B 3 wt% at high shear. We note that only 3 wt% of bentonite can produce mud with similar or more ideal rheological properties than those of 5 wt% by changing the manufacturing process. Considering the amount of mud used in the actual drilling industry, the amount of bentonite required for manufacturing can be reduced by 40 % compared with the current manufacturing practice. In this study, two processes for manufacturing bentonite particles on a nano-scale were reported, and both processes have a wide range of applications because they can be applied to a particle suspension containing particles.

5. Author's contribution

Hae Jin Jo and Sung Hyun Hong prepared equally experiment and wrote the original manuscript. Byung Min Lee measured size distribution of drilling muds. Young Ju Kim, Wook Ryol Hwang, and Soo Young Kim performed the data curation, overall review of the manuscript and funding acquisition. All authors read and approved the final manuscript.

CRediT authorship contribution statement

Hae Jin Jo: Conceptualization, Methodology, Writing – original draft. **Sung Hyun Hong:** Conceptualization, Methodology, Writing – original draft. **Byung Min Lee:** Data curation, Validation. **Young Ju Kim:** Supervision, Writing – review & editing. **Wook Ryol Hwang:** Supervision, Writing – review & editing. **Soo Young Kim:** Supervision, Writing – review & editing.

Declaration of Competing Interest

The authors declare that they have no known competing financial interests or personal relationships that could have appeared to influence the work reported in this paper.

Acknowledgments

This research was funded by the Korea Agency for Infrastructure Technology Advancement grant [grant number 22IFIP-C133622-06, 22IFIP-C133618-06, 22IFIP-C133614-06] funded by the Ministry of Land, Infrastructure, and Transport.

Appendix A. Supplementary data

Supplementary data to this article can be found online at https://doi.org/10.1016/j.ultsonch.2022.106246.

References

[1] B. Bloys, N. Davis, B. Smolen, L. Bailey, O. Houwen, P. Reid, M. Hodder, Designing and managing drilling fluid, Oilfield Rev. 6 (1994) 33–43.
[2] H.J. Skadsem, A. Leulseged, E. Cayeux, Measurement of drilling fluid rheology and modeling of thixotropic behavior, Appl. Rheol. 29 (2019) 1–11.
[3] K.V. Dyke, Drilling Fluid. Rotary Drilling Series. Unit 2, The University of Texas at Austin, 2000.
[4] J.E. Candler, J.H. Rushing, A.J.J. Leuterman, Synthetic-based mud systems offer environmental benefits over traditional mud systems. In: Paper presented at the SPE/EPA Exploration and Production Environmental Conference, San Antonio, Texas, March (1993) 485-499.
[5] M. Amani, M. Al-Jubouri, A. Shadravan, Comparative study of using oil-based mud versus water-based mud in HPHT fields, Adv. Pet. Explor. Dev. 4 (2012) 18–27.
[6] P.M. Hanson, T.K. Trigg, G. Rachal, M. Zamora, Investigation of barite "Sag" in weighted drilling fluids in highly deviated wells, in: Paper presented at the SPE Annual Technical Conference and Exhibition, New Orleans, Louisiana, September (1990) 223-230.
[7] J. Azar, G.R. Samuel, Drilling Engineering, Pennewell Corporation, 2007.
[8] R. Caenn, H. C. Darley, G.R. Gray, Composition and properties of drilling and completion fluids. Elsevier, Waltham, MA (2011) USA.
[9] R. Caenn, G.V. Chillingar, Drilling fluids: State of the art, J. Pet. Sci. Eng. 14 (3-4) (1996) 221–230.
[10] Z. Vryzas, V.C. Kelessidis, Nano-based drilling fluids: A review, Energies 10 (4) (2017) 540.
[11] P.F. Luckham, S. Rossi, The colloidal and rheological properties of bentonite suspensions, Adv. Colloid Interface Sci. 82 (1-3) (1999) 43–92.
[12] P. Coussot, F. Bertrand, B. Herzhaft, Rheological behavior of drilling muds, characterization using MRI visualization, Oil Gas Sci. Technol. 59 (1) (2004) 23–29.
[13] E.A. Al-Khdheeawi, D.S. Mahdi, Apparent viscosity prediction of water-based muds using empirical correlation and an artificial neural network, Energies 12 (2019) 3067.
[14] V.C. Kelessidis, R. Maglione, Yield stress of water-bentonite dispersions, Colloid. Surf. A-Physicochem. Eng. Asp. 318 (1-3) (2008) 217–226.
[15] A.A. Khalil, M.S. Adnan, Effect of mud rheology on cuttings' transport in drilling operations, IOP Conf. Ser.: Mater. Sci. Eng. 671 (2020), 012067.
[16] P. Kumar, P.C. Kapur, D.N. Saraf, Effect of zeta potential on apparent viscosity of settling suspensions, Colloid Polym. Sci. 253 (1975) 738–743.
[17] K.P. Hoelscher, S. Young, J. Friedheim, G. De Stefano, Nanotechnology application in drilling fluids. Offshore Mediterranean Conference and Exhibition. OnePetro, March (2013).
[18] A.M. Needaa, P. Peyman, A.H. Hamoud, A. Jamil, Controlling bentonite-based drilling mud properties using sepiolite nanoparticles, Petrol. Explor. Dev. 43 (2016) 717–723.
[19] S.M. Kutty, M. Kuliyev, M.A. Hussein, S. Chitre, H. Mustafa, G. Penny, C. Lelenwa, Well Performance improvement using complex nano fluids, in: Abu Dhabi International Petroleum Exhibition and Conference. OnePetro, November (2015).
[20] Y. Jung, M. Barry, J.K. Lee, P. Tran, Y. Soong, D. Martello, M. Chyu, Effect of nanoparticle-additives on the rheological properties of clay-based fluids at high temperature and high pressure. Proceedings of the AADE National Technical Conference and Exhibition, 2011.
[21] S. Ghanbari, E. Kazemzadeh, M. Soleymani, A. Naderifar, A facile method for synthesis and dispersion of silica nanoparticles in water-based drilling fluid, Colloid Polym. Sci. 294 (2016) 381–388.
[22] D.V. Kosynkin, G. Ceriotti, K.C. Wilson, J.R. Lomeda, J.T. Scorsone, A.D. Patel, J. M. Tour, Graphene oxide as a high-performance fluid-loss-control additive in water-based drilling fluids, ACS Appl. Mater. Interfaces 4 (2011) 222–227.
[23] J. Abdo, M.D. Haneef, Clay nanoparticles modified drilling fluids for drilling of deep hydrocarbon wells, Appl. Clay Sci. 86 (2013) 76–82.
[24] M. Sedaghatzadeh, A. Khodadadi, An improvement in thermal and rheological properties of water-based drilling fluids using multiwall carbon nanotube (MWCNT), Iran J. Oil Gas Sci. Technol. 1 (2012) 55–65.
[25] M.I. Abdou, A.M. Al-Sabagh, M.M. Dardir, Evaluation of Egyptian bentonite and nano-bentonite as drilling mud, Egypt J. Pet. 22 (1) (2013) 53–59.
[26] M. Sirait, N. Bukit, N. Siregar, Preparation and characterization of natural bentonite in to nanoparticles by co-precipitation method, in: AIP conference proceedings (Vol. 1801, No. 1, p. 020006). AIP Publishing LLC, January (2017).
[27] K.S. Suslick, Sonochemistry, Science 247 (1990) 1439–1445.
[28] Z. Darvishi, A. Morsali, Synthesis and characterization of Nano-bentonite by sonochemical method, Ultrason. Sonochem. 18 (1) (2011) 238–242.
[29] Y. Nagasaka, A. Nagashima, Absolute measurement of the thermal conductivity of electrically conducting liquids by the transient hot-wire method, J. Phys. E: Sci. Instrum. 14 (12) (1981) 1435–1440.
[30] S. Barakan, V. Aghazadeh, Synthesis and characterization of hierarchical porous clay heterostructure from Al, Fe-pillared nano-bentonite using microwave and ultrasonic techniques, Microporous Mesoporous Mater. 278 (2019) 138–148.
[31] X. Bian, Y.J. Cui, L.L. Zeng, X.Z. Li, Swelling behavior of compacted bentonite with the presence of rock fracture, Eng. Geol. 254 (2019) 25–33.
[32] R.O. Afolabi, E.O. Yusuf, C.V. Okonji, S.C. Nwobodo, Predictive analytics for the vipulanandan rheological model and its correlative effect for nanoparticle modification of drilling mud, J. Pet. Sci. Eng. 183 (2019), 106377.
[33] T.C. Papanastasiou, Flows of materials with yield, J. Rheol. 31 (1987) 385–404.
[34] E. Mitsoulis, Flows of viscoplastic materials: Models and computations, Rheol. Rev. Br. Soc. Rheol. (2007) 135–178.
[35] T. Kamiya, M. Kaminoyama, K. Nishi, R. Misumi, Scale-up factor for mean drop diameter in batch rotor-stator mixers, J. Chem. Eng. Japan 43 (2010) 326–332.
[36] E.L. Paul, V.A. Atiemo-Obeng, S.M. Kresta, Handbook of Industrial Mixing: Science and Practice (2003) 710–742.
[37] F. Barailler, P.A.T. Heniche, CFD analysis of a rotor-stator mixer with viscous fluids, Chem. Eng. Sci. 61 (2006) 2888–2894.
[38] A.B. Metzner, R.E. Otto, Agitation of non-Newtonian fluids, AIChE J. 3 (1957) 3–10.